Studying the Crystallization of Polyoxometalates from Colloidal Softoxometalates

Article in Crystal Growth & Design · May 2018

DOI: 10.1021/acs.cgd.8b00443

6 authors, including:

Preethi Thomas
Indian Institute of Science Education and Research Kolkata

Shubham Chandel
École Polytechnique

Apabrita Mallick
Indian Institute of Science Education and Research Kolkata

Sreejith S. Sreekumar
Cochin University of Science and Technology

Article

Studying the Crystallization of Polyoxometalates from Colloidal Softoxometalates

Preethi Thomas, Shubham Chandel, Apabrita Mallick, SS Sreejith, Nirmalya Ghosh, and Soumyajit Roy

Cryst. Growth Des., **Just Accepted Manuscript** • DOI: 10.1021/acs.cgd.8b00443 • Publication Date (Web): 30 May 2018

is published by the American Chemical Society. 1155 Sixteenth Street N.W., Washington, DC 20036

Studying the Crystallization of Polyoxometalates from Colloidal Softoxometalates

*Preethi Thomas[ab], Shubham Chandel[c], Apabrita Mallick[ab], SS Sreejith[ab], Nirmalya Ghosh[c] and Soumyajit Roy[ab]**

[a]Eco-friendly Applied Materials Laboratory, College of Chemistry, Central China Normal University, 152 Luoyu Road, Wuhan, 430079 Hubei, P. R. China. Email: s.roy@mail.ccnu.edu.cn

[b]Eco-friendly Applied Materials Laboratory Materials Science Centre, Department of Chemical Sciences, Indian Institute of Science Education and Research- Kolkata, Mohanpur-741246, Nadia, West Bengal, India. Email: s.roy@iiserkol.ac.in

[c]Bio-Optics and Nanophotonics Laboratory, Department of Physical Sciences, Indian Institute of Science Education and Research-Kolkata, Nadia, West Bengal, India-741246. Email: nghosh@iiserkol.ac.in

KEYWORDS: Soft oxometalates, Polyoxometalates, Mueller Matrix polarimetry, Crystallization, Phase study, Colloids.

ABSTRACT: Understanding crystallization of polyoxometalates is challenging. The chemistry of the reactive oxometalates renders any physical modelling impossible as it is not clear how the speciation in solution occurs. In this study we circumvent this problem by using a model system of ammonium heptamolybdate tetrahydrate which has robust molecular structure and shows phase changes from true solution to colloidal softoxometalates (SOMs) to crystals as a function of concentration or volume fraction without any chemical change (problem of speciation) in the system. Temperature and ionic strength variation studies have been conducted with respect to volume fraction to construct a phase diagram showing the transitions from true solution to colloidal SOMs to crystals. The stabilization of the SOM phase has been shown to take place via the established counter ion condensation model in colloidal oxometalates. Transition from colloidal to crystalline phase has been observed at volume fractions of 0.1 and 0.19 at elevated temperature. These phase transitions have been studied using laser set up of Mueller matrix polarimetry, Raman spectroscopy, ESI-MS. The crystallization of polyoxometalates from colloidal SOM phase has been tested at the corresponding volume fractions by measurement of the osmotic compressibility of colloidal SOM phase by light scattering using Baxter type model. The study thus puts forward a clear picture in the matter of crystallization of polyoxometalates. When chemical speciation does not occur in the system, oxometalates form colloids or the SOM phase which undergoes phase transition to crystalline (polyoxometalate) POM phase. This study thus leads to the immediate causal conclusion that all polyoxometalate crystallizations are in fact phase transitions from colloidal (SOM) to crystalline phase once the chemistry of speciation is complete. Hence understanding the colloidal SOM phase in detail could lead to crystal engineering of the POMs in a facile and controlled manner.

INTRODUCTION

A typical synthesis of a polyoxometalate would involve acidification of an aqueous solution of an oxometalate salt followed by acidification and reduction in an alterable sequence.[1-6] Their self-assembly into equilibrium colloidal architecture would involve another series of complex maneuvers. Hence in the present synthetic context the proposition of a colloidal mixture as a mother-liquor for all polyoxometalates sound outlandish if not unsophisticated. However the history of polyoxometalate discoveries and developments follow exactly the reverse trajectory. First colloids of polyoxometalates were obtained[7, 8] much later their structures were obtained with the development of crystallography[3, 9-13]. Hence the evolution of science has in itself the idea that simple acidification and reduction of metal oxides would form a colloid. Based on the kinetic arrest parameters (pH, temperature and ionic strength) different crystals of clusters would be isolated. In principle these clusters could in turn be re-dispersed into a solution or a colloid to be more precise. However studying the phenomenon of this colloidal crystallization is complex. The reason is as follows. Most of the studies on crystallization of polyoxometalates have systems that are chemically active. Hence application of the concept of a thermodynamic equilibrium does not hold good. On the other hand the concepts of crystallization of colloids are based on systems that are chemically inert and hence the laws of thermodynamics can be tested on such systems. Thus the challenge in testing the proposition that mother-liquor for crystallization of polyoxometalates are essentially colloidal soft-oxometalates, lies in choosing a system of crystallization that has all the qualifications of polyoxometalates but is not chemically reactive. With this end in view we here demonstrate crystallization of ammonium heptamolybdate based system that shows transition from a molecular solution to colloidal soft-oxometalates and then to crystalline polyoxometalates as a function of concentration. Using the well-established theory of counter-ion condensation proposed earlier[14] we have shown that indeed there exists a colloidal phase of soft-oxometalates [4-6, 15-21] in this system that in turn with the increase in volume fraction (concentration) undergoes a phase-transition to polyoxometalates. The colloidal phase has been studied in detail using light scattering and Mueller matrix polarimetry (MMP).[22] Thereafter in lines with the proposed transition of colloidal oxometalates to crystalline polyoxometalates by adopting Baxter model [23-26] we have investigated the phenomenon of phase transition in this system using MMP and light scattering techniques. Here we demonstrate that with the change in volume fraction the system of colloidal SOMs based on heptamolybdates undergoes a phase transition to form crystalline polyoxometalates. Before we describe our experimental results in detail to demonstrate that indeed colloidal phases precede crystalline phases in the matter of polyoxometalate crystallization we review the literature in this context to put our work in the perspective of ongoing polyoxometalate and crystallization of colloids research.

Polyoxometalate research has primarily focused on molecular pathway for the formation of polyoxometalates. For instance, we have recently shown that starting from the solution of aqueous heptamolybdate how clusters of $\{Mo_{132}\}$ is formed.[27] Likewise the works of Poblet and Cronin has shown the formation various molecular pathways for the formation of different polyoxometalates.[28-30]. In the context of colloid research works of Odijk and Prinsen has shown how it is possible to apply optimized Baxter model[23-26] to understand crystallization of colloids primarily in the context of proteins and at times in the matter of polyoxometalates.[31] Very recently Nyman *et.al* have described crystallization of ferrihydroxides.[32] However bridging the gap of molecular and colloid chemistry insights in the matter of rigorous understanding of polyoxometalate crystallization from the stand-point of colloid science is still missing. We believe with this paper we bridge this gap. Now we describe our experimental design and results in details.

EXPERIMENTAL SECTION

Materials and Reagents. Commercially available ammonium heptamolybdate tetrahydrate salt and sodium chloride from Merck were used to prepare all aqueous dispersions of different weight percent and for ionic strength studies, respectively.

Preparation of {Mo_7} Dispersions. The weight percent of ammonium heptamolybdate tetrahydrate was varied from 0 to 50% in water to prepare dispersions for phase studies.

Phase Diagram studies. For studying the different phases in heptamolybdate species as a function of concentration, we varied weight percent of {Mo_7} from 1 to 50 % in water and heated to a temperature where either the system turned to a true solution or a stable dispersion. The colloidal nature of the SOM dispersion was confirmed from impinging laser light on it followed by Mueller Matrix studies.

Dynamic Light Scattering. In order to experimentally establish the linear relationship between the size of heptamolybdate colloidal rods with increasing relative permittivity of the medium, DLS measurements of {Mo_7} soft oxometalate dispersions were carried out in acetone-water mixture with the percent of acetone varying from 0% to 20 % (volume percent) in water. The average size distribution data was obtained from dynamic light scattering measurements using a Malvern Zetasizer instrument.

Scanning Electron Microscopy. Different weight percent solutions/dispersions (0% to 30%) of ammonium heptamolybdate tetrahydrate in water were diluted and then dropcast on silicon wafers. After drop-casting, the wafers were dried in a dust-free solvent evaporation chamber for further imaging. The SEM images were recorded with a SUPRA 55 VP-41-32 Scanning Electron Microscope and analysed by using the SmartSEM version 5.05 Zeiss software.

Mueller Matrix Polarimetry.

The experimental system[33] consists of a Xenon lamp (white light source), lenses as collimating optics, polarization state generator (PSG) unit, sample compartment, polarization state analyzer unit (PSA) and a spectrograph for the spectrally resolved signal detection. PSG unit consist of a fixed linear polarizer P1 (aligned horizontally with respect to lab frame) and a rotating achromatic quarter wave plate (QWP_1) as a combination to generate the required four (optimized) elliptical polarization states. The optimized elliptical polarization states were generated by sequentially orienting the axis of QWP1 to 35 ^{o}, 70 ^{o}, 105 ^{o} and 140 ^{o} with respect to the polarizer P1. The PSA unit consists of the same system but arranged in reverse order (rotating quarter wave plate QWP2 and then polarizer P2). The axis of the polarizer P2 (part of PSA) is fixed orthogonal to the polarizer P1. QWP_2 is consecutively oriented to the same angles as QWP1 to analyze these four elliptical states. The backscattered light from sample is collected using a lens and collimated using an assembly of lenses, then passed through the PSA unit, and is finally recorded using a spectrometer (Figure 1). The recorded sixteen measurements were used to construct full 4×4 spectral Mueller matrices with the combination of PSG and PSA. During the measurements, few μL (~5-10) of sample solution was transferred to a cuvette with 0.1 cm breadth and 1.0 cm path length. The complete 4x4 Mueller matrix were recorded for the wavelength range of 500 to 700 nm with spectral resolution of 2.0 nm. The complete system is automated using Labview for fast acquisition and hustle free recording. The details of this system can be found elsewhere too.[33] The developed system was accurately calibrated using a Eigen Value Calibration (ECM) method. It compensates for the wavelength dependence, non-ideal behavior of optical components, misalignments and etc. as explained elsewhere.[34] The Mueller matrix was further decomposed using polar decomposition technique[35] to extract the quantified polarimetric parameters named diattenuation (differential amplitude of orthogonal polarizations), Retardance (phase difference of the orthogonal polarization components) and depolarization (loss of degree of polarization). These polarimetric parameters are then utilized for the quantification of phase change of heptamolybdate species in water with varying weight percentages (volume fractions).

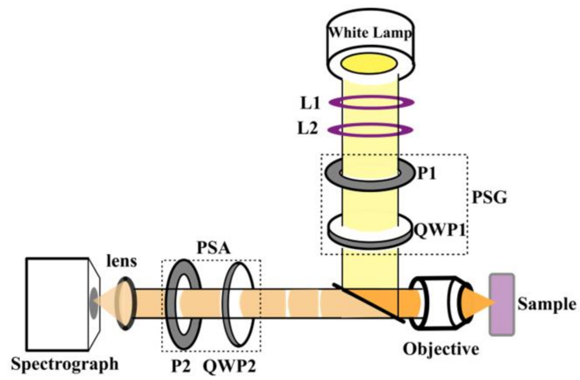

Figure 1. The schematics of the spectral Mueller matrix polarimetry set-up used to record the full 4x4 spectral Mueller matrix.

THEORY

Stokes-Mueller Algebra used in Mueller Matrix Polarimetry:

Here, we briefly introduce the concept of Mueller matrix and its inverse analysis. The polarization state of light is presented by four measurable quantities known as Stokes vector when grouped in a 4×1 vector (I, Q, U, V are the elements of the Stokes vector **S**). While the Stokes vector engraves the polarization properties of light, Mueller Matrix contains complete information about all the polarization properties of the interacting medium. Please note the Mueller matrix polarimetry is different from the conventional polarimetry where excitation and detection using selected linear polarization states are used.[22] Such conventional polarimetry methods provide only limited information and several crucial information are masked, whereas Mueller matrix polarimetry provides the complete polarization information. In short, the 4×4 Mueller Matrix is a mathematical description of the polarization altering interaction of light with a medium exhibiting intrinsic polarimetry characteristics,

$$\mathbf{S}_o = \mathbf{M}\ \mathbf{S}_i$$

Where $\mathbf{S}_i$ and $\mathbf{S}_o$ are the input and the output Stokes vectors, respectively. Various schemes have been developed to record 4×4 Mueller matrix of any medium. As discussed above, we have utilized an in-house developed automated spectral 4×4 Mueller Matrix measurement system[i] (Figure 1), to record the full spectral (wavelength 500 – 700 nm) Mueller Matrix from the solutions. All the sample polarization properties are encoded in various elements of the Mueller matrix. The three basic polarization properties that are encoded in Mueller matrix are diattenuation, retardance and depolarization.[22] Diattenuation is defined as differential attenuation of orthogonal linear polarizations (between horizontal / vertical or between +45 deg/-45 deg, accordingly termed as linear diattenuation) and orthogonal circular polarizations (between left and right, circular diattenuation). Retardance property on the other hand, deals with phase shifts between orthogonal linear polarizations (linear retardance) and circular polarizations (circular retardance or optical rotation). The third polarization property, depolarization refers to loss of polarization due to randomization of polarization (e.g, by multiple scattering events). For samples exhibiting multiple polarization effects that too in presence of scattering (as is the case for the samples studied here), the recorded Mueller matrix represent 'lumped' effects resulting in inter element cross talk, masking potentially interesting intrinsic polarization metrics. In order to extract and quantify the constituent polarimetry effects, the recorded Mueller matrix was then decomposed using polar decomposition technique to yield the individual intrinsic polarimetry characteristics. Using this approach, the recorded Mueller Matrix of any complex system is decomposed as the product of three basis matrices:

$$\mathbf{M} \Leftarrow \mathbf{M}_{\Delta} \bullet \mathbf{M}_{R} \bullet \mathbf{M}_{D}$$

Here, the matrix $\mathbf{M}_R$ contains the retardance effect (both circular and linear), $\mathbf{M}_D$ expresses the effect of linear and circular diattenuation, $\mathbf{M}_{\Delta}$ describes the depolarizing effects of the medium. This decomposition technique was proposed by Lu and Chipman.[35]

From the decomposed matrices, the relevant polarization parameters, depolarization (Δ), diattenuation (D) and linear retardance (δ) are quantified as:

$$\Delta = 1 - \frac{|Tr(M_{\Delta}) - 1|}{3}$$

$$D = \frac{1}{M_{D(1,1)}}\sqrt{M_D(1,2)^2 + M_D(1,3)^2 + M_D(1,4)^2}$$

$$\delta = \cos^{-1}\left\{\sqrt{[M_R(2,2) + M_R(3,3)]^2 + [M_R(3,2) - M_R(2,3)]^2} - 1\right\}$$

RESULTS AND DISCUSSION

Phase Diagram Studies

1. **Ternary Phase Diagram Studies**:

It is known that ammonium heptamolybdate forms molecular solution with water even at room temperature. However our earlier investigations show that they form colloidal soft-oxometalate phases as well. Hence to understand the location of soft-oxometalates and polyoxometalates as a function of oxometalate concentration, temperature and water concentration a ternary phase diagram was constructed (Figure 2).

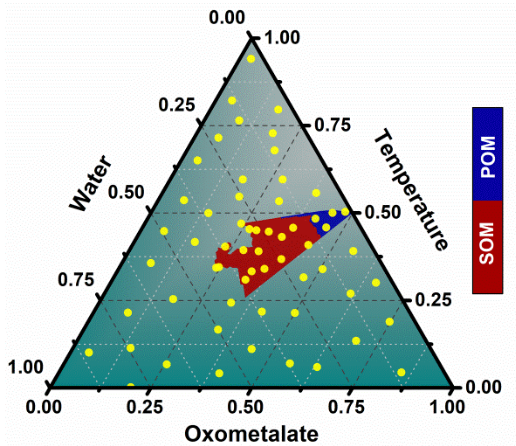

Figure 2. Ternary phase diagram showing transition from true solution to colloidal SOM to crysralline POM. volume fraction of oxomolybdate (0-0.35) and water (0-100%) and temperature (30-90^{0}C) have been normalized. The region marked in maroon denotes the soft-oxometalate (SOM) phase and the blue region denotes crystalline POM formed from SOM.

In Figure 2 we have plotted the volume fraction of ammonium heptamolybdate and water with respect to the temperature as a three-coordinate system. The volume fraction of oxomolybdate (0-0.35) and water (0-100%) and temperature (30-90^{0}C) have been normalized and scaled as 0-1. Different amount of oxomolybdate was dispersed in different volumes of water and heated at different temperatures. 55 sample dispersions (shown by the yellow points) were taken and their phase was observed to construct the ternary phase diagram. The temperature is restricted to 85^{0}C (below boiling point of water) as from the TGA plot (Figure S1, supplementary information) it is observed heptamolybdate starts losing water of crystallization beyond 100^{0}C. The region marked in maroon denotes the soft-oxometalate (SOM) phase. With gradual increase in volume fraction of the heptamolybdate in water the crystalline POM starts forming from the SOM phase which is marked by the blue region in the phase diagram. Behavior of heptamolybdate species in water in different weight percentages are shown in Figure S3, supplementary information.

From the ternary phase diagram it emerges that in the matter of heptamolybdates the crystalline phase emerges (where oxometamalate = 0.41, temperature = 0.4, water = 0.1 in the plot) as a transition from colloidal SOM state to crystalline POM state. It also appears that the POM phase is nested within the SOM phase prompting us to propose that crystallization of POMs proceeds via a colloidal state of SOMs. Now we investigate the microscopic nature of the SOM and the POM phases in more microscopic details as a function of weight percentage (volume fraction) and temperature. Ammonium heptamolybdate tetrahydrate shows different phases at different weight percent (Volume fraction) in water which we have shown in the form of a phase diagram (Figure 2). In the lower concentration regime, i.e. from1% to 9% weight percent (volume fraction of 0.01-0.09), there was no scattering of laser light thus demonstrating true solution behavior of these species below temperature of 70^0C . However, within the temperature range of 30-60°C, and at weight percentage of 7.5% to 8% (volume fraction 0.075-0.08) Ammonium heptamolybdate tetrahydrate scatter light and show soft matter properties such as scattering of light. At 60°C, weight percentage of 9% (volume fraction of 0.09) a true solution with no scattering is observed. At 70°C, and weight percentage of 10% (volume fraction 0.1) a stable dispersion of SOM state is observed.

Microscopic investigations show that in this state Ammonium heptamolybdate tetrahydrate predominantly exist as rod-shaped particles that constitute colloidal soft oxometalates. These colloidal forms are at first detected by light scattering characteristics and by Mueller matrix polarimetry studies which also reveals that these particulate structures are not crystalline and are colloidal in nature. The details of Mueller matrix studies have been elaborated in the next section. The colloidal SOM regime extends till weight percentage of 19% (volume fraction 0.19) at 75°C where we observe a phase transition from colloidal soft oxometalates to crystalline state of Ammonium heptamolybdate tetrahydrate. It is to be noted that at lower temperature range between 20-40 °C, and with lower weight percentages lesser than 19% we also observe crystalline phases. For instance, at 20 °C, and at weight percentage of 15 % (volume fraction 0.15) we observe crystalline phases. In turn these studies again point to the existence of POM phases as transitions from SOM phases. To prove that heptamolybdate remains the same at all volume fractions we performed Raman spectroscopy (Figure S4, supplementary information) and ESI-MS (Figure S5, supplementary information) studies which confirm that heptamolybdate remains unchanged during the investigations[27]. Now we investigate with MMP the phase transitions in more details.

Phase studies using Mueller Matrix Polarimetry:

In order to investigate the phase change for the Ammonium heptamolybdate tetrahydrate in detail three different weight percentages from different phase states of the above phase study (5%, 15%, 30%) were subjected to the Mueller matrix studies. The 4x4 scattering Mueller matrices were recorded for each of the weight percentage. The first element of the recorded Mueller Matrix corresponds to the total intensity. The presented Mueller matrix (in this case) is normalized with first (M11) element. The diagonal elements mainly reveal the depolarization effect (loss of polarization) due to multiple scattering and randomization of polarization vector.

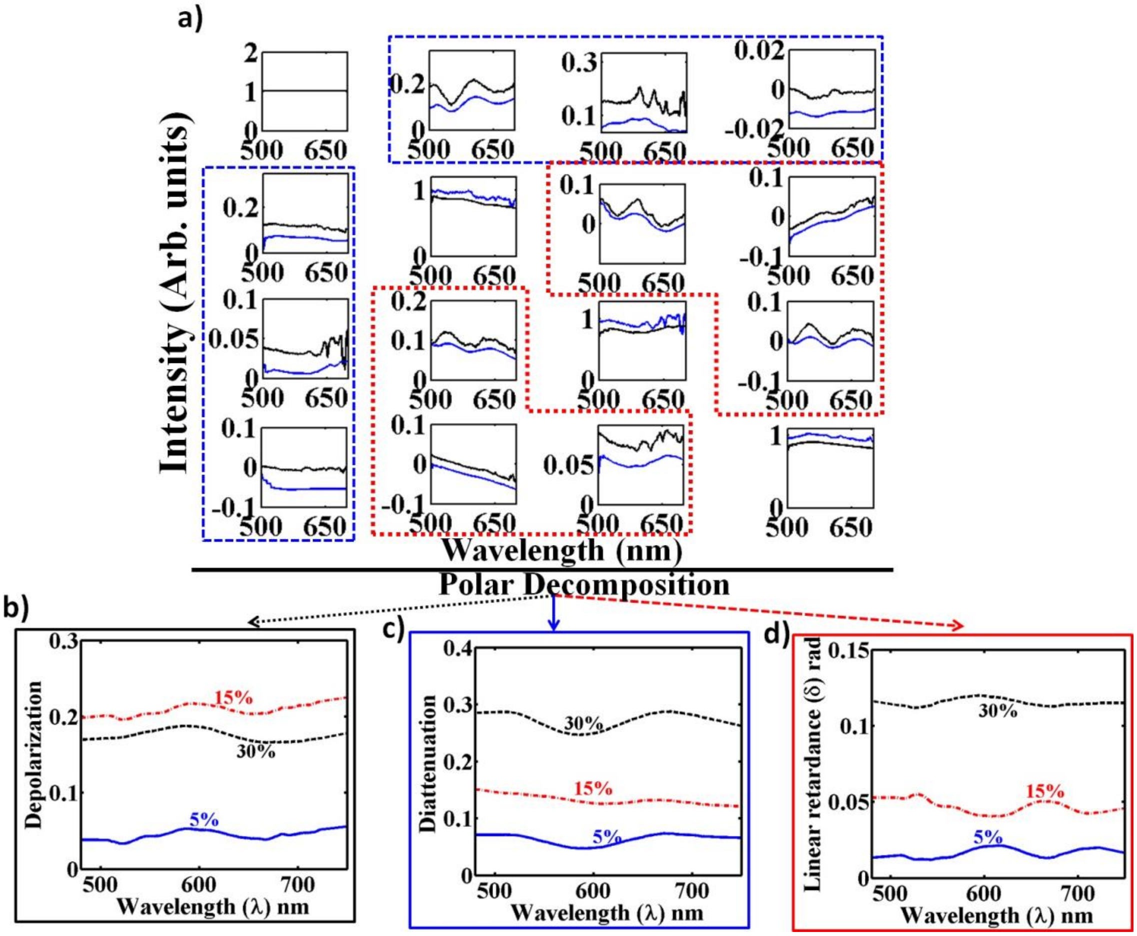

Figure 3. (a) Spectral Mueller matrix for two phase/weight percentage (Blue for true solution, red for colloidal SOM phase and black for crystalline phase) **(b)** Depolarization, **(c)** Diattenuation, **(d)** Linear Retardance obtained from Mueller matrix polarimetry for true solution, SOM phase and crystalline phase at weight percentage of 5%, 15% and 30% of Ammonium heptamolybdate tetrahydrate.

Higher the magnitude of the diagonal elements, lesser is the loss of polarization which corresponds to diminished multiple scattering or lesser randomization of polarization vector (similar to the case of true solution lacking any loss of polarization). The elements M24, M42, M34 and M43 (shown with red dots) primarily illustrate the phase retardance effect. The lower values of the above mentioned elements will lead to lowered magnitude of retardance parameter which is the typical characteristics of phase randomization, similar to the case of true solution phase of {Mo_7} which will have almost negligible phase retardance as reflected from these Mueller matrix elements. The 1st row and 1st column elements of the Mueller matrix (shown with a blue dotted box) principally determine the diattenuation property of the medium. The higher magnitude of these elements corresponds to higher magnitude of diattenuation parameter, demonstrating organized structure/orientation effects like the crystalline phase {Mo_7} as represented by the 1st row and column elements of the recorded Mueller matrix. The recorded Mueller matrix is decomposed to extract and quantify the three basic polarization effects, which will effectively probe and quantify the phase change. The decomposed parameters for three different weight percentages are shown in Figure 3.

As expected for the true solution case (1-9%), the diattenuation, linear retardance and depolarization parameters showed very low value. The true solution will have very weak multiple scattering thus giving rise to close to zero depolarization value whereas for the colloidal state (i.e. from 7.5% to 19%) the multiple scattering will be quite strong. As mentioned above, stronger randomization of polarization (caused by multiple scattering) would give rise to higher depolarization. The higher weight percent (higher volume fraction) of Ammonium heptamolybdate tetrahydrate i.e. beyond 19% is in crystalline phase. Crystalline phase being more organized, will lead to lesser multiple scattering thus lesser randomization, as a result lesser depolarization w.r.t colloidal state. The diattenuation and retardance parameters relate to the anisotropy of the organization, where diattenuation representing amplitude anisotropy and retardance encoding phase anisotropies. Moving from true solution to colloidal to crystalline state the microscopic orientation of the system becomes more and more complex but macroscopically more organized. Such macroscopically organized state like of a crystalline state would offer higher anisotropies (amplitude and phase both). Such macroscopic anisotropic behavior is probed by the diattenuation and retardance parameter as can be seen in the Figure 3 c),d). The crystalline ammonium heptamolybdate tetrahydrate has organized structure and will therefore result in highest magnitude (w.r.t colloidal and true solution phase) for diattenuation and retardance, whereas for the true solution case the values are correspondingly negligible. The diattenuation and retardance parameter of the colloidal rods of ammonium heptamolybdate tetrahydrate will have slightly less magnitude (w.r.t crystalline form) due to their relatively less organized arrangement than what is observed in $\{Mo_7\}$ crystals. These results assert the phase change taking place in ammonium heptamolybdate tetrahydrate at various weight percent and is being probed using the three basic polarization parameters (depolarization, diattenuation and retardance) extracted from recorded spectral Mueller matrix.

Stabilization of Ammonium heptamolybdate tetrahydrate SOMs

Once the existence of multiple phases in ammonium heptamolybdate tetrahydrate was confirmed using Mueller matrix polarimetry and light scattering experiments, we tried to characterize the soft-oxometalate state in more details. From SEM images (Figure S6, supporting information), the rod like morphology of ammonium heptamolybdate tetrahydrate SOMs was confirmed. We further investigated the factors that contribute towards the stabilization of rod shaped self-assembly. At first we came up with an expression modified from earlier published counter-ion condensation model of Kegel group[18] for these colloidal ammonium heptamolybdate tetrahydrate rods wherein all the stabilizing and destabilizing factors were incorporated. We herein propose that the anionic part of heptamolybdate self-assembles to form a rod like arrangement stabilized by counter ion condensation of ammonium cations around the self-assembled heptamolybdate ions, $\{Mo_7O_{24}{}^{6-}\}$. The free NH_4^+ ions are prevented from approaching this arrangement due to the repulsive force exerted by the positively charged condensed ammonium ions around $\{Mo_7\}$ rods. Thus the rod-like structures are held together by short range repulsive forces and long range attractive forces. If we consider the rod shape of SOMs to be equivalent to a cylinder capped by two hemispheres at each end, the free energy expression for SOMs can be written as:

$$\frac{F}{kT} = (2\pi RL + 4\pi R^2)\gamma_0 + \frac{\pi KL}{R} + 4\pi\widetilde{K} + \frac{2\lambda_B}{kR(2R+L)}\frac{K_0(kR)Z^2}{K_1(kR)} - \Psi Z \qquad 1.$$

where F- Helmholtz Free Energy, k- Boltzmann constant, T-Temperature, R-radius of the cylinder with hemispherical ends, L- length of the cylinder with hemispherical ends, γ_0- surface tension, K- Elastic modulus, $\widetilde{K}$- Gaussian modulus, λ_B – Bjerrum length, $K_0(kR)$- Bessel function of the second kind and zero order, $K_1(kR)$- Bessel function of the second kind and first order. Ψ- zeta potential and Z- effective charge.

In equation 1, the first term on the right hand side denotes the surface tension term followed by second and third terms, both of which denote the contribution of curvature from Helfrich expansion. The fourth term stands for the screened Coulomb interaction while the fifth term denotes the extent of escape from the Gouy layer.

If we differentiate eq. 1 with respect to Z and minimize it, we get:

$$Z = \frac{\Psi kR(2R+L).K_1(kR)}{4\lambda_B K_0(kR)} \qquad 2.$$

Further, by substituting eq. 2 in eq. 1, we get:

$$\frac{F}{kT} = \frac{\pi KL}{R} + 4\pi\widetilde{K} - \Psi^2 kR(2R+L)\frac{K_1(kR)}{8\lambda_B K_0(kR)} \qquad 3.$$

If we differentiate eq. 3 with respect to the area of the spherocylinder we get:

$$\frac{L}{2R} = \frac{\Psi^2 kR^2\, K_1(kR)}{16\pi\lambda_B K_0(kR)} \qquad 4.$$

Eq. 4 shows the inverse proportionality relation between length and Bjerrum length, λ_B.

As λ_B can be expressed as:

$$\lambda_B = \frac{e^2}{4\pi\varepsilon_0\varepsilon_R kT} \qquad 5.$$

in terms of absolute and relative permittivity, ε_0 and ε_R, respectively.

Considering eq. 4 and 5, we get a direct proportionality relationship between the length and relative permittivity constant.

$\mathrm{L} \propto \varepsilon_R$

Thus it means that the length of the SOM rods increases with increasing dielectric constant. In order to confirm our theoretical proposition, we measured the length (manifest as hydrodynamic radius) of 10% SOMs in different ratios of acetone-water ranging from pure water to 20% acetone-water mixture, using dynamic light scattering. The different volume percent of acetone in water gave us the desired change in the dielectric constant of the medium. It is important to note here that due to the rod like morphology, the SOMs would undergo tumbling along their length in the light scattering experiments which means that the hydrodynamic radius, R_H obtained from the size distribution plot in DLS, would in fact be the length of the spherocylindrical SOM. In this manner, we can determine the length of the SOM rods in different media with varied polarity tuned by addition of acetone in water in different volume ratio. Once we plot the values of R_H versus dielectric constant, ε_R we observe a linear graph confirming the linear relationship between the two (Figure 4) thus substantiating our theoretical model of how SOMs are formed and stabilized.

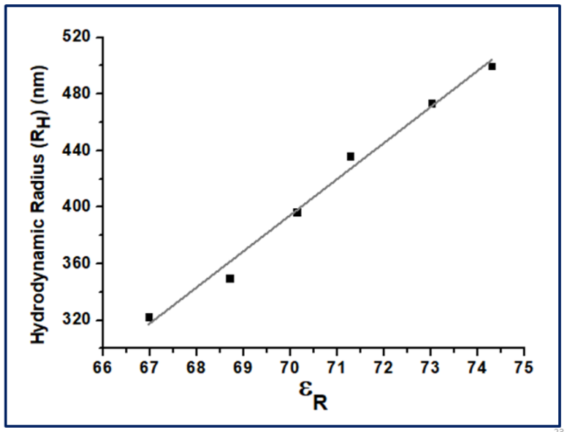

Figure 4. The plot between hydrodynamic radius, R_H obtained from dynamic light scattering experiments and dielectric constant, ε_R.

Variation of Ionic Strength Studies:

Ammonium heptamolybdate is 1:6 electrolyte where 6 NH_4^+ are the countercations and we can calculate the ionic strength (I) using the formula, $I = \frac{1}{2}\,\Sigma c_i z_i^2$ where c_i is the molar concentration and z_i is the charge number of the i^{th} ion. With increasing volume fraction of the heptamolybdate the ionic strength also increases. Debye length (κ^{-1}) of colloid is inversely proportional to the square root of the ionic strength and can be related by the equation $\kappa^2 = 8\pi QI$ and the Bjerrum length $Q = q^2/\epsilon k_B T$ where q is the elementary charge and ϵ is the permittivity of water. For the colloidal SOM regime (volume fraction 0.1-0.19), the double layer between two particles persists and from the figure κ^{-1} is found to be ranging between 5-10 nm. In a crystal, the particles are positionally ordered and the double layers are forced to overlap and the value of κ^{-1} becomes very small (<5 nm, from figure 5(A)). Thus the phase separation from colloidal SOM to crystalline POM with increasing ionic strength of heptamolybdate is evident from the graph.

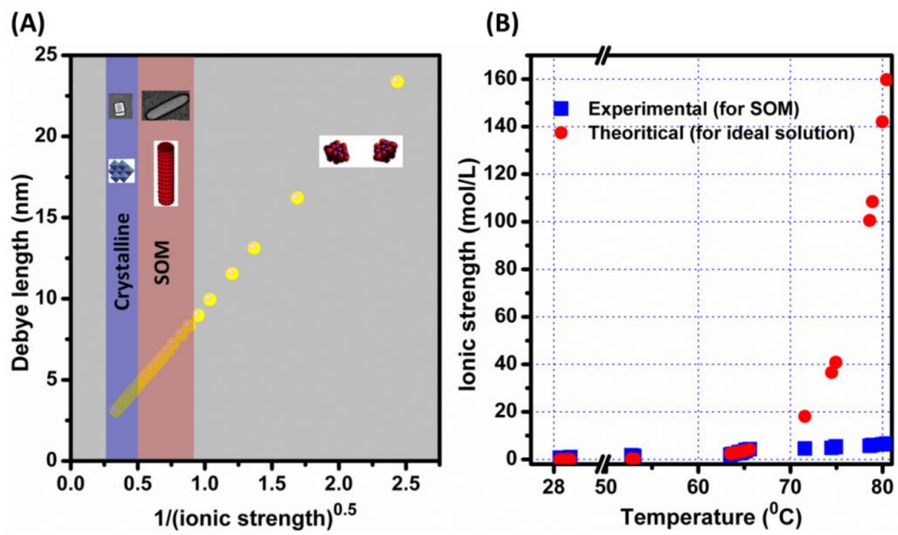

Figure 5. (A) Plot of Debye length vs 1/(ionic strength)$^{0.5}$ showing phase transition from SOM to POM. **(B)** Plot showing comparison between ionic strengths of SOM and ideal solution at different temperatures.

We also compared the experimental ionic strength (I) of heptamolybdate in aqueous dispersions from the above formula and compared them with the ionic strength of heptamolybdate in ideal solution (obtained theoretically, Figure 5(B)). For ideal solutions, the molar fraction of heptamolybdate can be calculated from the equation $\ln N = -\frac{L_f}{R}(\frac{1}{T} - \frac{1}{T_m})$ where N = mole fraction of the heptamolybdate, L_f is the molal heat of fusion of heptamolybdate, T_m is the melting point of the solute in K. L_f is again calculated from $T_m = T_0 - \frac{RT_0^2}{L_f}.\frac{1}{F}$

From TGA and DSC of heptamolybdate (Figure S1, supplementary information), $T_m = 124^0C$ and $T_0 = 90^0C$, F = 7/100. Calculated value of L_f is 236 kJ mol^{-1}. At lower temperature range (30-65^{0}C), the theoretical values of ionic strength of ideal solutions match well with the experimental values of heptamolybdate solutions. But at temperature 70^{0}C and above, the experimental value of ionic strength are much less as compared to that of ideal solutions. This deviation appears due the formation of colloidal SOM at higher temperatures. Low ionic strengths implicate that the colloidal SOMs are stabilized via charge regulation as well as counterion condensation.

Osmotic Compressibility Measurements

In the colloidal regime of soft oxometalates, the positively charged ammonium counter ion layer around heptamolybdate anions prevents entry of nearby ammonium ions, thereby acting as a semi permeable membrane which selectively prohibits intrusion of positive ions. In a given medium say, water, an osmotic pressure is generated across this counter ion encapsulation. The osmotic compressibility is the second coefficient of the virial expansion series and is denoted χ_T. Following literature we propose that in this case as χ_T is overcome, it leads to the phase separation of the SOM rod-like assemblies to form crystalline heptamolybdate POMs.

In our work, we have attempted to measure this osmotic compressibility with the simple scattering measurement set-up (Figure S2, supplementary information). We employ a 631.4 nm helium neon laser source and shine light on 19% $\{Mo_7\}$ dispersion (since we observe phase transition of SOMs to POMs at this weight percent). The scattered intensity is collected by a convex lens which is passed over to a detector (fixed on a rotating stage along with collection lens) to measure the intensity at different angles.

The osmotic compressibility, χ_T of a system can be expressed as,

$$\chi_{T=}\frac{R}{N_a k T c_p^2 K} \qquad 1.$$

where, $$K = \frac{4\pi^2 n^2}{\lambda^4 N_a}\left(\frac{\partial n}{\partial c_p}\right)^2 \qquad 2.$$

N_a- Avogadro number = 6.022 X 10^{23}

k- Boltzmann constant = 1.38 X 10^{-23} m^2 kg s^{-2} K^{-1}

T- Temperature = 298 K

n- Refractive index =1.33

c_p- Molar concentration of 19% weight percent of {Mo_7} = $\frac{1.9\ X\ 100}{1235.86}$ = 0.1537 M

V- Scattering volume = $\pi r^2 h = 3.14\ X\ 1^2 X\ 10$ = 31.4 mm^3 = 3.14 X 10^{-8} m^3

and $$R = \frac{I_{out}}{I_0}.\frac{|r|^2}{V} \qquad 3.$$

with output intensity as I_{out}, initial intensity I_0 , radius, r of the cylindrical laser beam.

By assuming there is no substantial change in the refractive index of the medium with respect to change in concentration of heptamolybdate i.e., $\frac{\partial n}{\partial c_p} = 1$ and by substituting the values of K and R from equation 2. and 3., respectively in equation 1., we get:

$$\chi_{T=}\frac{I_{out}}{I_0}.\frac{|r|^2}{V}\frac{\lambda^4}{4\pi^2 n^2 k T c_p^2} \qquad 4.$$

We obtain the $\frac{I_{out}}{I_0}$ value from the experimental set up shown in Figure S2 to be around 0.0884. By substituting the values for each of the variables in equation 4, we can compute the osmotic compressibility of heptamolybdate at 19% weight percent. χ_T is calculated to be 1.137 X 10^{-13} Pa^{-1}. We note the osmotic compressibility at the crystallization boundary is indeed comparable to the value published in literature. This measurement in conjugation with MMP and phase studies indeed shows that at osmotic compressibility of 1.137 X 10^{-13} Pa^{-1} there is a phase transition from the colloidal state to crystalline state.

CONCLUSION

In summary, we have presented the panorama of molecular solution of ammonium heptamolybdate tetrahydrate forming colloidal soft-oxometalate cylinders and finally forming crystalline state of polyoxometalates as a function of weight percentage/volume fractions. Confirmation and validation of three phases (SOM phase, colloidal phase and crystalline phase) of ammonium heptamolybdate tetrahydrate formed at different weight percent (volume fractions) is obtained from microscopy, light scattering and Mueller matrix polarimetry studies. The rod like assemblies of ammonium heptamolybdate tetrahydrate was observed in the colloidal SOM phase which is shown to be stabilized by counterion condensation. We have further shown the transition from the SOM phase to the crystalline phase and have measured the osmotic compressibility of the colloidal SOMs at 19% weight percent that leads to its transition to crystalline phase and the value was determined to be 1.137 X 10^{-13} Pa^{-1}. The formation, stabilization and phase transition in ammonium heptamolybdate tetrahydrate SOMs was studied and efficiently probed using Mueller matrix polarimetry. In short this study shows that in case of ammonium heptamolybdate tetrahydrate, true solution phase, colloidal SOM phase and crystalline POM phases can be traversed as a function of weight percentage (volume fraction). The study further implies that colloidal SOM phase precedes crystalline POM phase. It is thus reasonable to propose that crystallization of all POMs proceed via the mother-liquor of SOMs and it is worth investigating those SOMs from the standpoint of colloid science and Mueller matrix polarimetry to understand and predict crystallization of POMs.

ASSOCIATED CONTENT

Supporting Information. TGA-DSC graphs, schematic representation of the set-up used for measuring osmotic compressibility of ammonium heptamolybdate SOMs, photographs of heptamolybdate species in water in different weight percents, raman spectroscopic studies of the heptamolybdate at different weight percentage, negative ion mode ESI-MS spectrum for aqueous dispersions of heptamolybdate, SEM images of the heptamolybdate dispersions . This material is available free of charge via the Internet at http://pubs.acs.org.

The following files are available free of charge.

Online supporting information

AUTHOR INFORMATION

Corresponding Author

***E-mail:** s.roy@mail.ccnu.edu.cn, s.roy@iiserkol.ac.in

Author Contributions

The manuscript was written through contributions of all authors. All authors have given approval to the final version of the manuscript. PT, SC and AM contributed equally

Funding Sources

SR acknowledges the financial support of DST Fast track, BRNS DAE, India and Start up and FIRE grants from IISER-Kolkata, India.

Notes

The authors declare no competing financial interest.

REFERENCES

(1) Müller, A.; Serain, C., Soluble molybdenum blues "des pudels kern". *Acc. Chem. Res* **2000,** 33, (1), 2-10.

(2) Müller, A.; Diemann, E.; Kuhlmann, C.; Eimer, W.; Serain, C.; Tak, T.; Knöchel, A.; Pranzas, P. K., Hierarchic patterning: architectures beyond 'giant molecular wheels' Dedicated to Professor Phillip Gütlich on the occasion of his 65th birthday. *ChemComm* **2001**, (19), 1928-1929.

(3) Kistler, M. L.; Bhatt, A.; Liu, G.; Casa, D.; Liu, T., A Complete Macroion−"Blackberry" Assembly− Macroion Transition with Continuously Adjustable Assembly Sizes in {Mo132} Water/Acetone Systems. *J. Am. Chem. Soc* **2007,** 129, (20), 6453-6460.

(4) Roy, S., "Soft Oxometalates"(SOMs): A Very Short Introduction. *Comments Inorg. Chem.* **2011,** 32, (3), 113-126.

(5) Roy, S., Soft-oxometalates beyond crystalline polyoxometalates: formation, structure and properties. *CrystEngComm* **2014,** 16, (22), 4667-4676.

(6) Crans, D. C.; Roy, S., Introduction for the Emergent Polyoxometalates and Soft-oxometalates thematic issue. *New J. Chem* **2016,** 40, (2), 882-885.

(7) Scheele, C. W., Sämtliche Physische und Chemische Werke. In Hermbstädt, D. S. F. ed.; Martin Sändig oHG, Niederwalluf/Wiesbaden, 1971: 1971 (reprint from 1793 original); Vol. 1, pp 185-200.

(8) Berzelius, J. J., Beitrag zur näheren Kenntniss des Molybdäns. *Annalen der Physik* **1826,** 82, (4), 369-392.

(9) Pope, M. T.; Müller, A., Polyoxometalate chemistry: an old field with new dimensions in several disciplines. *Angew. Chem. Int. Ed* **1991,** 30, (1), 34-48.

(10) Liu, T.; Diemann, E.; Li, H.; Dress, A. W.; Müller, A., Self-assembly in aqueous solution of wheel-shaped Mo 154 oxide clusters into vesicles. *Nature* **2003,** 426, (6962), 59.

(11) Pradeep, C. P.; Misdrahi, M. F.; Li, F. Y.; Zhang, J.; Xu, L.; Long, D. L.; Liu, T.; Cronin, L., Synthesis of modular "inorganic–organic–inorganic" polyoxometalates and their assembly into vesicles. *Angew. Chem. Int. Ed* **2009,** 48, (44), 8309-8313.

(12) Schreiber, R. E.; Houben, L.; Wolf, S. G.; Leitus, G.; Lang, Z.-L.; Carbó, J. J.; Poblet, J. M.; Neumann, R., Real-time molecular scale observation of crystal formation. *Nat. Chem.* **2017,** 9, (4), 369.

(13) Mani, E.; Sanz, E.; Roy, S.; Dijkstra, M.; Groenewold, J.; Kegel, W. K., Sheet-like assemblies of spherical particles with point-symmetrical patches. *J. Chem. Phys.* **2012,** 136, (14), 144706.

(14) Verhoeff, A. A.; Kistler, M. L.; Bhatt, A.; Pigga, J.; Groenewold, J.; Klokkenburg, M.; Veen, S.; Roy, S.; Liu, T.; Kegel, W. K., Charge regulation as a stabilization mechanism for shell-like assemblies of polyoxometalates. *Physical review letters* **2007,** 99, (6), 066104.

(15) Barman, S.; Das, S.; Sreejith, S.; Garai, S.; Pochamoni, R.; Roy, S., Selective Light Driven Reduction of CO2 to HCOOH in Water Using {MoV9} n (n= 333-900) Based Soft-oxometalate (SOM). *ChemComm* **2018,** 54, 2369-2372.

(16) Das, S.; Biswas, S.; Balaraju, T.; Barman, S.; Pochamoni, R.; Roy, S., Photochemical reduction of carbon dioxide coupled with water oxidation using various soft-oxometalate (SOM) based catalytic systems. *J. Mater. Chem. A* **2016,** 4, (22), 8875-8887.

(17) Das, S.; Kumar, S.; Garai, S.; Pochamoni, R.; Paul, S.; Roy, S., Softoxometalate [{K6. 5Cu (OH) 8.5 (H2O) 7.5} 0.5@{K3PW12O40}] n (n= 1348–2024) as an Efficient Inorganic Material for CO2 Reduction with Concomitant Water Oxidation. *ACS Appl. Mater. Interfaces* **2017,** 9, (40), 35086-35094.

(18) Das, S.; Thomas, P.; Roy, S., Photoinduced Topological Transformation in Mesoscopic Inorganic Nanoparticles: Application as a UV Sensor. *Eur. J. Inorg. Chem.* **2014,** 2014, (27), 4551-4557.

(19) Mallick, A.; Lai, D.; Roy, S., Autonomous movement induced in chemically powered active soft-oxometalates using dithionite as fuel. *New J. Chem* **2016,** 40, (2), 1057-1062.

(20) Roy, B.; Arya, M.; Thomas, P.; Jurgschat, J. K.; Venkata Rao, K.; Banerjee, A.; Malla Reddy, C.; Roy, S., Self-assembly of mesoscopic materials to form controlled and continuous patterns by thermo-optically manipulated laser induced microbubbles. *Langmuir* **2013,** 29, (47), 14733-14742.

(21) Das, K.; Roy, S., Direct Synthesis of Controlled- Size Nanospheres inside Nanocavities of Self- Organized Photopolymerizing Soft Oxometalates [PW12O40] n (n= 1100–7500). *Chem. Asian J.* **2015,** 10, (9), 1884-1891.

(22) Gupta, S. D.; Ghosh, N.; Banerjee, A., *Wave optics: Basic concepts and contemporary trends*. ed.; CRC Press: 2015.

(23) Prinsen, P.; Odijk, T., Optimized Baxter model of protein solutions: Electrostatics versus adhesion. *J. Chem. Phys.* **2004,** 121, (13), 6525-6537.

(24) Prinsen, P.; Pàmies, J. C.; Odijk, T.; Frenkel, D., Application of the optimized Baxter model to the hard-core attractive Yukawa system. *J. Chem. Phys.* **2006,** 125, (19), 194506.

(25) Prinsen, P.; Odijk, T., Collective diffusion coefficient of proteins with hydrodynamic, electrostatic, and adhesive interactions. *J. Chem. Phys.* **2007,** 127, (11), 09B615.

(26) Prinsen, P.; Odijk, T., Fluid-crystal coexistence for proteins and inorganic nanocolloids: Dependence on ionic strength. *J. Chem. Phys.* **2006,** 125, (7), 074903.

(27) Biswas, S.; Melgar, D.; Srimany, A.; Rodríguez-Fortea, A.; Pradeep, T.; Bo, C.; Poblet, J. M.; Roy, S., Direct Observation of the Formation Pathway of [Mo132] Keplerates. *Inorg. Chem.* **2016,** 55, (17), 8285-8291.

(28) Vilà- Nadal, L.; Rodríguez- Fortea, A.; Yan, L. K.; Wilson, E. F.; Cronin, L.; Poblet, J. M., Nucleation mechanisms of molecular oxides: a study of the assembly–dissassembly of [W6O19] 2− by theory and mass spectrometry. *Angew. Chem. Int. Ed* **2009,** 48, (30), 5452-5456.

(29) Vilà-Nadal, L.; Mitchell, S. G.; Rodríguez-Fortea, A.; Miras, H. N.; Cronin, L.; Poblet, J. M., Connecting theory with experiment to understand the initial nucleation steps of heteropolyoxometalate clusters. *Phys. Chem. Chem. Phys.* **2011,** 13, (45), 20136-20145.

(30) Zheng, Q.; Vilà-Nadal, L.; Lang, Z.; Chen, J. J.; Long, D.-L.; Mathieson, J. S.; Poblet, J. M.; Cronin, L., Self-Sorting of Heteroanions in the Assembly of Cross-shaped Polyoxometalate Clusters. *J. Am. Chem. Soc* **2018,** 140, (7), 2595-2601.

(31) Rosenbaum, D.; Zamora, P.; Zukoski, C., Phase behavior of small attractive colloidal particles. *Phys. Rev. Lett* **1996,** 76, (1), 150.

(32) Sadeghi, O.; Zakharov, L. N.; Nyman, M., Aqueous formation and manipulation of the iron-oxo Keggin ion. *Science* **2015,** 347, (6228), 1359-1362.

(33) Soni, J.; Purwar, H.; Lakhotia, H.; Chandel, S.; Banerjee, C.; Kumar, U.; Ghosh, N., Quantitative fluorescence and elastic scattering tissue polarimetry using an Eigenvalue calibrated spectroscopic Mueller matrix system. *Opt. Express* **2013,** 21, (13), 15475-15489.

(34) De Martino, A.; Garcia-Caurel, E.; Laude, B.; Drévillon, B., General methods for optimized design and calibration of Mueller polarimeters. *Thin Solid Films* **2004,** 455, 112-119.

(35) Lu, S.-Y.; Chipman, R. A., Interpretation of Mueller matrices based on polar decomposition. *JOSA A* **1996,** 13, (5), 1106-1113.

For table of contents use only:

Studying the Crystallization of Polyoxometalates from Colloidal Softoxometalates

*Preethi Thomas[ab], Shubham Chandel[c], Apabrita Mallick[ab], SS Sreejith[ab], Nirmalya Ghosh[c] and Soumyajit Roy[ab]**

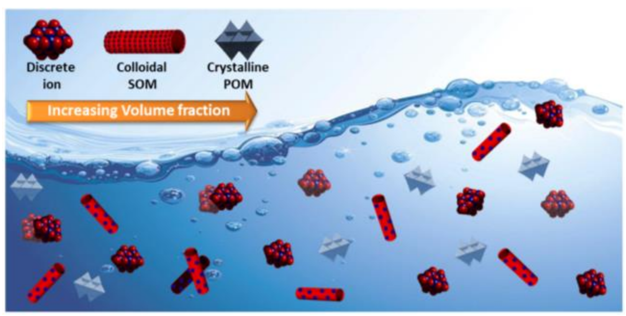

Phase transition from colloidal soft-oxometalates to crystalline polyoxometalates using a model system of heptamolybdate have been demonstrated with the help of Ternary phase diagram, Mueller Matrix Polarimetry and counter-ion condensation method.

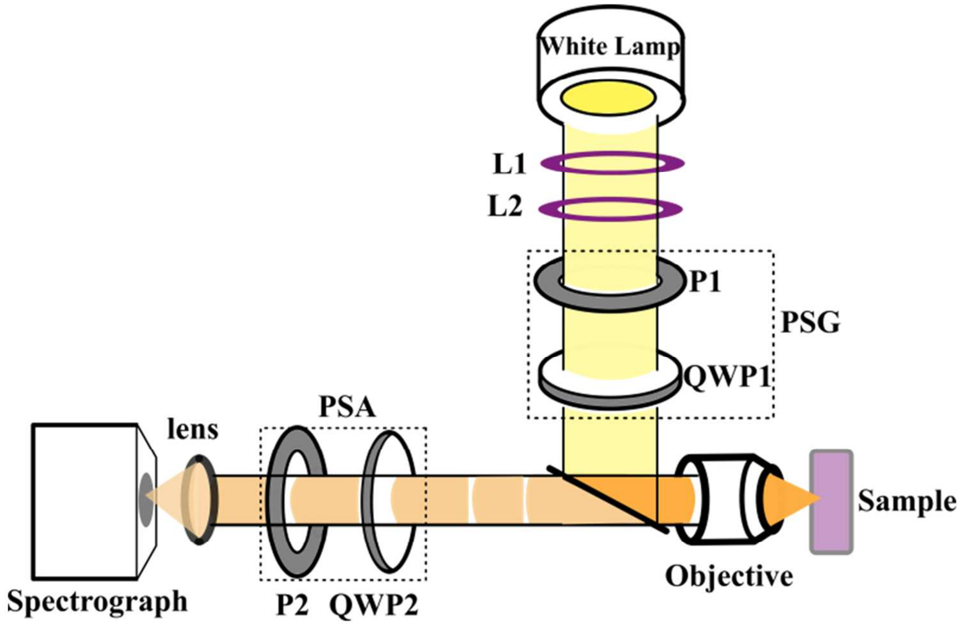

Figure 1. The schematics of the spectral Mueller matrix polarimetry set-up used to record the full 4x4 spectral Mueller matrix.

254x164mm (150 x 150 DPI)

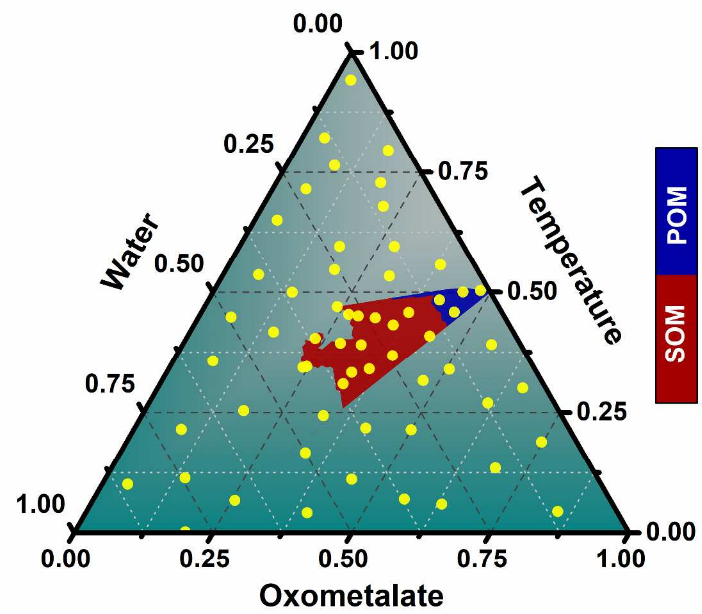

Figure 2. Ternary phase diagram showing transition from true solution to colloidal SOM to crysralline POM. volume fraction of oxomolybdate (0-0.35) and water (0-100%) and temperature (30-900C) have been normalized. The region marked in maroon denotes the soft-oxometalate (SOM) phase and the blue region denotes crystalline POM formed from SOM.

297x208mm (300 x 300 DPI)

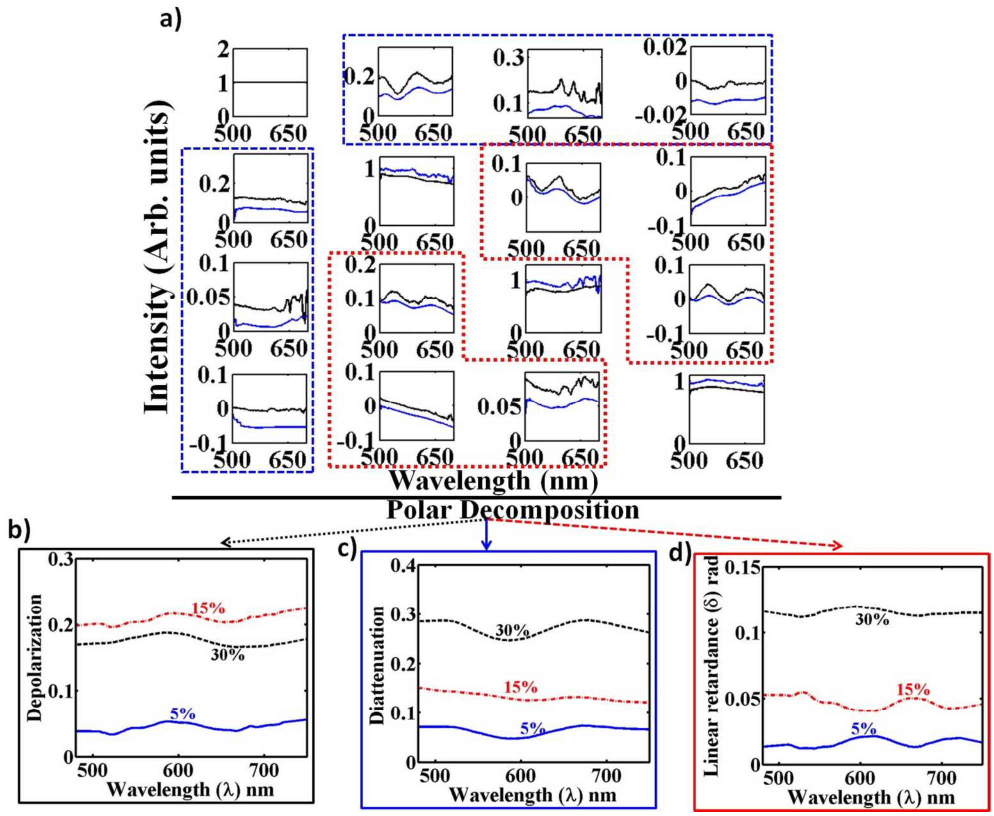

Figure 3. (a) Spectral Mueller matrix for two phase/weight percentage (Blue for true solution, red for colloidal SOM phase and black for crystalline phase) (b) Depolarization, (c) Diattenuation, (d) Linear Retardance obtained from Mueller matrix polarimetry for true solution, SOM phase and crystalline phase at weight percentage of 5%, 15% and 30% of Ammonium heptamolybdate tetrahydrate.

296x243mm (144 x 144 DPI)

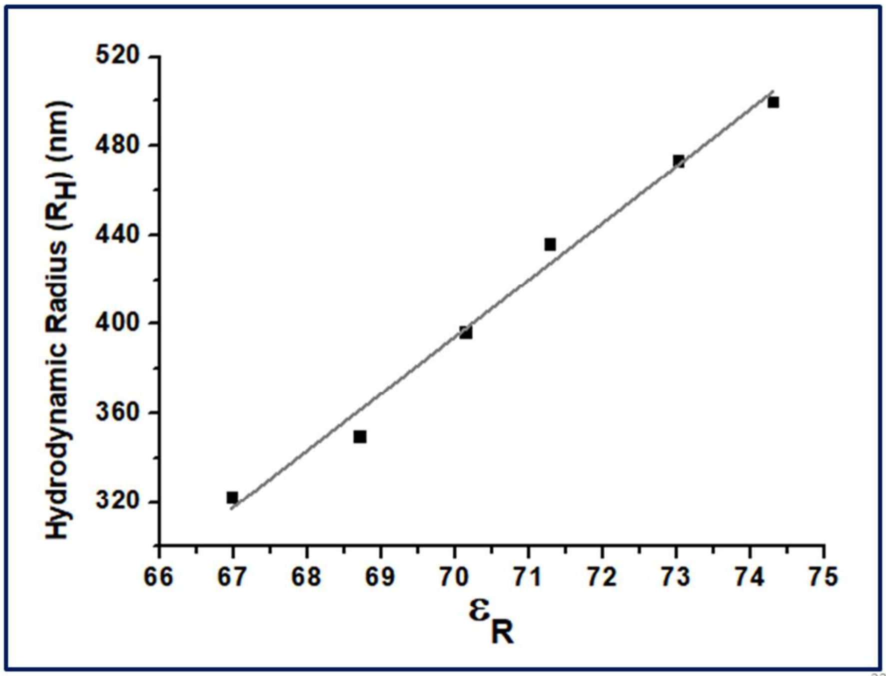

254x190mm (96 x 96 DPI)

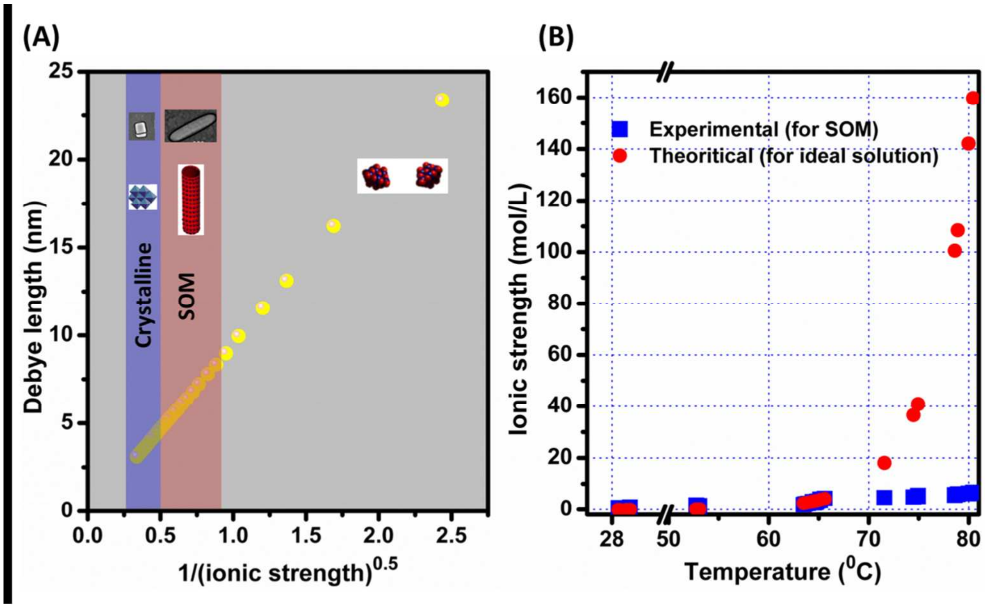

Figure 5. (A) Plot of Debye length vs 1/(ionic strength)0.5 showing phase transition from SOM to POM. (B) Plot showing comparison between ionic strengths of SOM and ideal solution at different temperatures.

159x95mm (220 x 220 DPI)